Lattice Excitations of the ^{4}He Quantum Solids*

V. J. Minkiewicz†
University of Maryland, College Park, Maryland 20740

T. A. Kitchens and G. Shirane
Brookhaven National Laboratory, Upton, New York 11973

E. B. Osgood
Stevens Institute of Technology, Hoboken, New Jersey 07030

(Received 12 January 1973)

Extensive inelastic-neutron-scattering experiments have been carried out on single crystals of ^{4}He in the bcc and low-density hcp phases. The results of our present and previous measurements have established the over-all characteristics of the scattering function $S(Q, \omega)$ for a wide range of energy and momentum transfers. The general features of the scattering function can be described as showing well-defined, sharp, elementary excitations at energy transfers $\hbar\omega < 1.0$ meV, and single-particle excitations for scattering vectors $|Q| > 3.0$ Å^{-1} and $\hbar\omega > 5.0$ meV. The changes in the structure of the scattering function to accommodate these two different excitations occur in an ill-defined "transition" region, wherein the spectral response of the sharp excitation gradually becomes more distorted and merges with the multiexcitation response at the higher energies. In the low-energy regime, the scattering cross section for sharp excitations observed in the [0$\bar{1}$1] zone for the bcc phase is found to be unusual in that the effective Debye-Waller factor constructed from the data via the Ambegaokar, Conway, and Baym sum rule displays oscillations. The data for the lowest transverse branch T_1, however, do not show oscillations. In our previous work, this anomalous cross section appeared to be associated with an energy transfer of $\sim$ 1.4 meV, and a concomittant distortion in the Gaussian-like spectral response. The present results show that this is not the case. The unexpected behavior of the cross section was observed for sharp, symmetric excitations whose energy distribution has no extraordinary contribution near 1.4 meV. The measurements in the hcp phase show that these anomalous features of the scattering function are similar in both phases. The high-resolution measurements on the sharp excitations at small wave vector were used to construct a self-consistent set of elastic constants. These elastic constants are considerably more accurate than those from previous measurements. They suggest that the dispersion of the T_1 mode in the [011] direction need not be anomalous, in contrast to recent theoretical results. Finally, at high energy and momentum transfers, single-particle excitations are observed in both phases. Their dispersion relation is isotropic, and is the same in both phases within the accuracy of the measurements. The profiles of these excitations are very similar to those recently observed by Woods and Cowley in the superfluid phase.

I. INTRODUCTION

For large molar volume the solids of ^{4}He have the unique feature that, in contrast to normal systems, the average random excursion of an atom from its equilibrium position is a significant fraction ($\sim\frac{1}{3}$) of the interatomic spacing. The weak interatomic interaction and the light mass combine to produce crystals whose lattice dynamics cannot be described within the context of classical theory.[1] For these reasons, and because the interatomic interaction is well known, helium crystals are expected to be ideal systems with which to test the subtle predictions of the quantum-mechanical many-body theory of crystal dynamics.

In recent years the over-all experimental effort on inelastic neutron scattering from helium crystals has made considerable progress. The initial work on single-crystal samples was done in the hcp phase by the Brookhaven group[2] for a molar volume of 21.1 cm^3/mole and by the Ames group[3] at 16.0 cm^3/mole. Their results for the dispersion curves are in reasonable agreement with theory. There were, however, two puzzling features in the experiments. The first was that the higher-energy LO branches were not observed by the Brookhaven group for the large-molar-volume crystal of 21.1 cm^3/mole. The second was that Reese *et al.*[3] noted that occasionally they observed "anomalous neutron groups" that could not be reliably identified as the standard single-phonon scattering. With regard to the measurements made at the larger molar volume, it was speculated that the LO branches were not observed because of relaxation effects and because the inelastic structure factor had an unexpected dependence on the scattering vector. These two aspects of the experiments had, however, never been satisfactorily resolved, and remain unsolved problems.

It was therefore highly desirable to perform

measurements in the other low-density phase of ^{4}He, the bcc phase. The initial experiments were done in the hcp phase because of the more formidable cryogenic problems in the bcc. The problem of stabilizing a crystal in this phase for approximately one month is difficult, since it exists over a temperature interval of at most 50 m°K. Our experiments on the bcc phase were reported by Osgood *et al.*,[4] hereafter referred to as I. The results of these experiments can be summarized as follows: (i) With regard to the dispersion curves, where possible, the agreement between theory and experiment[4] was of the order of ±20%; (ii) the group profiles in the higher-energy region of the phonon spectrum were often severely distorted from the normal Gaussian contour; (iii) the profiles of the groups were not identical at symmetry-related positions in reciprocal space; (iv) the first moments of the groups near $|Q| \sim 2.5$ Å^{-1} were not in agreement with the sum rule developed by Ambegoakar, Conway, and Baym,[5] assuming that the Debye-Waller factor had the expected Gaussian dependence on the length of the scattering vector. The data shown in Fig. 1 were taken from I, and illustrate that an unexpected increase in the scattering function had occurred for $|Q| \sim 2.4$ Å^{-1}. It was also concluded that the anomaly is associated with an energy transfer of ~1.4 meV and a distortion in the group profiles.

This experiment generated a great deal of interest, and many attempts were made to explain the results.[6-9] Werthamer[6] has suggested that the anomaly might be understood on the basis of the solid being more liquidlike than expected. The observed distorted profiles and the difference in their shape at symmetry-related positions are taken to be evidence for strong interference effects in the single-phonon scattering function.

Sears and Khanna,[7] McMahan and Guyer,[8] and Horner[9] approached the problem differently and studied the behavior of the Debye-Waller factor from the Hartree-Jastrow approximation, the self-consistent phonon approximation[1] (SCH), and improvements on the SCH, respectively. They failed to reproduce the data for the anomaly in the scattering function. The dependence of the theoretical Debye-Waller factor on the magnitude of the scattering vector was found to be Gaussian to within 2%, and the directional dependence too small to explain the result. Sears and Khanna[7] had even suggested that "the anomaly" is due to errors in background subtractions.

Further experiments were therefore necessary, both to clarify questions raised by the early measurements and to study the anomaly in more detail. In particular, it was recognized that extensive measurements on low-energy excitations

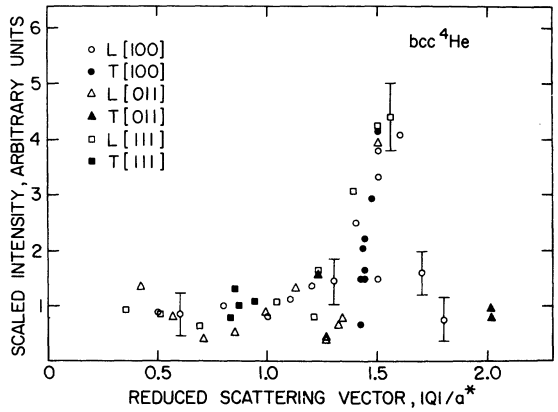

FIG. 1. Results for the intensity anomaly given in Ref. 4. The cross section for $|Q| \sim 1.6a^*$ is too large by approximately a factor of 4.0. If conventional theory were correct, the data would be independent of $|Q|$ and lie on the straight line. Scaled intensity = 1.0.

($\hbar\omega < 1.0$ meV) would be important because they could be studied with high resolution. The previous measurements were restricted to an incident-neutron energy of 13.5 meV, which in turn made reciprocal space near zone centers inaccessible. In this paper we will demonstrate that the anomalous behavior of the scattering function is not associated with an energy transfer of 1.4 meV, and does not occur in only those groups that are distorted. The unexpected cross section, as will be shown, was observed in sharp excitations with a symmetrical spectral response where there is no difficulty with background subtraction. In addition, we shall show that for $\hbar\omega > 5.0$ meV and $Q > 3.0$ Å^{-1}, there exist single-particle-like excitations.[10]

II. PRELIMINARY COMMENTS

A. Experimental Details

The experimental results that are given in this paper are a composite of data collected from five different crystals. The crystals had a nominal volume of 8 cm^3. The mosaic of the samples typically had a smooth Gaussian-like profile with a full width at half-maximum (FWHM) of 10′, with a shoulder that was between 10 and 50% of its peak height. The shoulders extended to at most 0.5° from the peak of the profile. In principle, the presence of the shoulder presents no difficulty; the data could easily be corrected for it. However, it was decided to study the transverse branches only in the best crystals, for which the corrections are small. The longitudinal branches, being much less affected by crystal mosaic, were studied in all the crystals. The data were completely consistent from one crystal to the next.

A detailed description of the procedure used to grow the crystals is given in I; here we will mention only two features of the sample cell not mentioned there. Because the sample-cell fill line is restrictive (a 20-cm-long 0.01-cm-i.d. capillary containing an 0.008-cm wire), a pump-out value was provided for evacuating the sample cell before Dewar assembly. Because this restrictive filling line was susceptible to blockage, the sample cell also was equipped with a miniature bursting disk with a bursting pressure of about 40–50 atm. Both the pump-out value and the bursting-disk assembly are superfluid tight even at elevated pressures, and are described in detail elsewhere.[11]

The scattering vectors that are normally used to collect phonon dispersion data for cubic crystals are fairly standard and well known. The unusual restrictions imposed by the Debye-Waller factor of solid helium, however, are unique, and require the use of scattering geometries not ordinarily considered. The positions at which the data were collected for bcc helium in these experiments are illustrated in Fig. 2. The scattering vectors were chosen to sample only propagation vectors along the major symmetry directions, for which the polarization vectors of the modes are fixed by symmetry to be either transverse or longitudinal. Crystals oriented in two zones were used. The majority of the data was taken on crystals oriented in a $[0\bar{1}1]$ zone. All but one of the important branches can be studied in this zone, the exception being the lowest transverse mode T_1 along the [011] direction. The polarization of this mode is along the $[0\bar{1}1]$ direction and to study this mode a crystal oriented in a [100] zone was used.

The data were collected using fixed incident energies of 5.5, 13.7, and 44.0 meV. The constant-Q scan technique was used for the experiments. The lower incident energies were used for energy transfers generally less than 4.0 meV. In those cases where very clean high-resolution data were necessary, an incident energy of 5.5 meV was used; the energy transfer was then limited to less than 1.1 meV. The monochromator and analyzer were (002) reflections of pyrolytic graphite. The higher-energy components in the beam were eliminated by using graphite as a single-crystal filter. Effective collimations of 20′ were used before and after the scattering from the sample. The incident energy of 44.0 meV was used to study the high-energy single-particle excitations. The energy transfer in this case was between 5.0 and 20 meV. Again, the (002) reflection of pyrolytic graphite was used at the analyzer and monochromator positions.

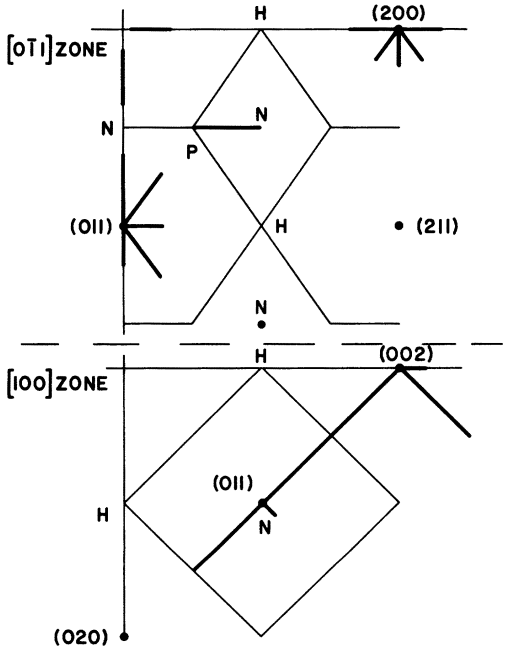

FIG. 2. Two zones in which crystals were oriented in the bcc phase. The heavy solid lines illustrate the positions where the data were collected.

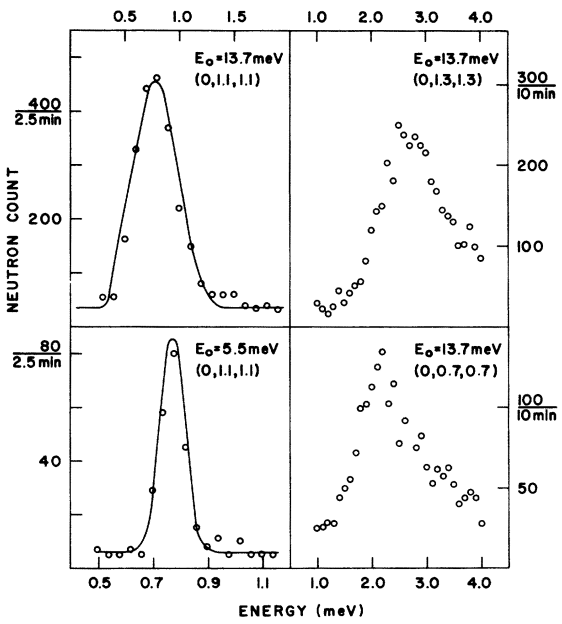

FIG. 3. Four examples of scans in the bcc phase. The two scans on the right illustrate the shift in apparent peak position and marked difference in intensity of groups taken at two equivalent positions in reciprocal space. The two scans on the left are examples of the same phonon being taken with incident energies of 13.7 and 5.5 meV.

B. Scattering Function

To simplify the discussion of the experimental results in Sec. IV we give here a preliminary over-all preview of the characteristics of the scattering function for low-density solid helium. The traditional interpretation given to inelastic neutron scattering from a solid was not fully adequate to describe the data. The profiles shown in Fig. 3 illustrate the three principal types of features observed in the scattering function.

The profile on the lower left is a representative example of the data collected with high resolution at energy transfers less than 1.1 meV. The solid lines in the figure are the result of a computer calculation that convolutes the resolution function of the spectrometer with the dispersion curves of bcc helium as determined by a force-constant fit. The cross section used in the convolution assumed that these excitations were infinitely long lived. The fact that the solid lines in the figure faithfully reproduce the data indicates that the observed linewidth of these excitations is primarily caused by the resolution of the instrument. An upper limit for their intrinsic width can be fixed at approximately $\frac{1}{3}$ of the observed FWHM, or ~0.03 meV. The data given in Fig. 3 are typical of those observed for the lowest-lying peak in the spectral response at low-energy transfer, and can, we believe, be identified with confidence as scattering from the elementary lattice excitations. The results for neutron groups of this type can therefore be compared with the theoretical results for the dispersion curves, as is usually done.

The situation for higher-energy transfers is considerably more complex. The two profiles on the right-hand side of the figure are typical of the data taken at higher energies. These data were collected at equivalent positions in reciprocal space, and should be compared with one another. In addition to their both being very broad, we note that their profiles are different. With regard to this difference in their profiles, it is known that the terms introduced into the scattering cross section by the interference between the one-phonon and multiple-phonon background can produce precisely this result.[5] The important feature, however, is not that their profiles are different, but rather that the cross section at the [0, 1.3, 1.3] position is too large to be entirely conventional single-phonon scattering. The increase in the cross section at the higher-energy transfers and for the large scattering vectors is evidence that the single-excitation response is being masked and often dominated by an additional contribution to the scattering function. We shall refer to this additional contribution as multiple-excitation scattering. In a later section, we shall show that the profile given in the upper right "becomes" the single-particle scattering at even higher energies.[10]

These results suggest that the data be discussed as though there are three regions in energy and momentum space. In the first, the scattering function shows a sharp well-defined spectral response characteristic of a long-lived elementary excitation; the second is an ill-defined transition region wherein the multiple- and single-excitation responses become superposed to such an extent that separation of the two becomes impossible; finally, there is the region for very-high-energy transfers and large scattering vectors, where the scattering function is determined by the single-particle response. In addition it is clear that in the transition region the conventional concept of the dispersion relation is of limited use, and that the proper method of analyzing the results is generally not by assigning "peak positions" and widths but by detailed computer convolution of the spectrometer resolution function with theoretical results for the total scattering function $S(\vec{Q}, \omega)$. The theoretical calculations are unfortunately nontrivial. However, a quantitative comparison between theory and experiment in the transition region of the excitation spectrum of solid helium should prove to be especially interesting.

C. Sum Rules

When presenting the experimental results, emphasis will be placed on the magnitude of the cross section. We now comment on the manner in which the data are reduced. One way to discuss the cross section for an elementary lattice excitation is via the sum rule on the displacement-displacement correlation function developed by Ambegaokar, Conway, and Baym (ACB).[5] The ACB sum rule asserts that

$$\int_{-\infty}^{+\infty} d\omega\, \omega S_p^i(\vec{Q}, \omega) = \frac{(\vec{Q}\cdot\vec{\xi}_i)^2 |d(\vec{Q})|^2}{2M}\,, \tag{1}$$

where $S_p^i(\vec{Q}, \omega)$ is the so-called single-phonon scattering function for branch i with polarization vector ξ_i, $\vec{Q}$ is the scattering vector, ω is the energy transfer, and $|d(\vec{Q})|^2$ is the Debye-Waller factor. We note that $S_p^i(\vec{Q})$ contains the cross terms alluded to earlier: namely, the interference terms introduced by the one-phonon and multiphonon scattering amplitudes. Detailed balance can be used to restrict the integral in Eq. (1) to phonon creation to give

$$\int_0^{\infty} d\omega\, \omega S_p^i(\vec{Q}, \omega)(1 - e^{-\beta\omega}) = \frac{(\vec{Q}\cdot\vec{\xi}_i)^2 |d(\vec{Q})|^2}{4M}, \tag{2}$$

where $\beta = \hbar/kT$. If the integral in Eq. (2) is defined to be $M_i^1(\vec{Q})$, we note that it can be constructed from the data. Then either $M_i^1(\vec{Q})$, $M_i^1(\vec{Q})/(\vec{Q}\cdot\vec{\xi}_i)^2$, or $M_i^1(\vec{Q})/(\vec{Q}\cdot\vec{\xi}_i)^2 e^{-2W_h}$ can be used to present the experimental results, where e^{-2W_h} is the harmonic Debye-Waller factor. These three equivalent ways of presenting the results are schematically illustrated in Fig. 4. The dashed lines in the figure illustrate what one would have for the coherent single-phonon cross section using the normal Gaussian Debye-Waller approximation, $|d(\vec{Q})|^2 = e^{-2B(Q/4\pi)^2}$. The solid lines qualitatively illustrate, as will be seen, what is actually observed for the scattering from solid helium. In I the results were presented after the fashion given in the top part of the figure. In this paper we shall use both the top and the bottom presentations.

The data that were given in I have appeared in the literature plotted in a fourth fashion.[6] The quantity $M_i^1/(\vec{Q}\cdot\vec{\xi})^2$ was plotted on a linear scale versus $|Q|$; in other words, one gets a linear plot of the effective Debye-Waller factor. This type of plot can possibly be misleading. The important feature contained in the data given in I is that the intensity of the scattering at $|Q| \sim 2.44$ Å^{-1} was much too large. A linear plot of the effective Debye-Waller factor could be interpreted as emphasizing more the region $|Q| \sim 1.2$ Å^{-1}, rather than the additional cross section at 2.44 Å^{-1}. The data were given in I after the fashion given in the top part of Fig. 4 to illustrate that the unambiguous experimental result was an unexpected *increase* in the cross section at 2.44 Å^{-1}.

The illustration given in the bottom part of Fig. 4 is particularly instructive. The solid line A in the figure represents what one would get if *all* the scattering were contained in the observations. It represents Placzek's[12] sum rule on the total scattering function,

$$\int_{-\infty}^{+\infty} d\omega\, \omega S(\vec{Q}, \omega) = Q^2/2M, \tag{3}$$

where $S(\vec{Q}, \omega)$ is the total scattering function. The figure clearly suggests that one might immediately anticipate difficulties in uniquely identifying the single-phonon part of the scattering in the transition region. The dashed line represents the contribution made by the single-phonon part in the harmonic approximation. For Q small, the single-phonon part dominates. The difference between the line A and the dashed line represents the contribution made by the multiple-phonon part, which becomes progressively larger. In the extreme limit for Q very large, namely, in the single-particle region, one should reproduce the line A exactly. In the transition region the two contribute amounts of equal order, and a clear separation of the two becomes virtually impossible. As was discussed earlier, the experimental results support this conclusion. We now proceed to present a detailed description of the scattering function for solid helium in all three regions of energy and momentum space.

III. DISPERSION CURVES

A. bcc Phase

We first discuss the data that were taken in the region in which the scattering function has a simple profile that can readily be identified as scattering from a single elementary excitation. Two examples of typical high-resolution scans taken in this region are illustrated in Fig. 5. The excitations shown in the figure are sharp and well defined. An upper limit for their intrinsic linewidth is approximately $\frac{1}{3}$ of the observed FWHM, or ~0.03 meV. The results for the dispersion curves for small wave vector are summarized in Fig. 6. Data of the type shown in Fig. 5 were used to determine the elastic constants. The solid lines in Fig. 6 are the least-squares fit to the data that give the elastic constants in Table I of the Appendix. The data for five branches, the $T[100]$, $L[011]$, $T_2[011]$, $L[111]$, and $T[111]$, were used in the least-squares analysis. The results for the T_1 branch were taken

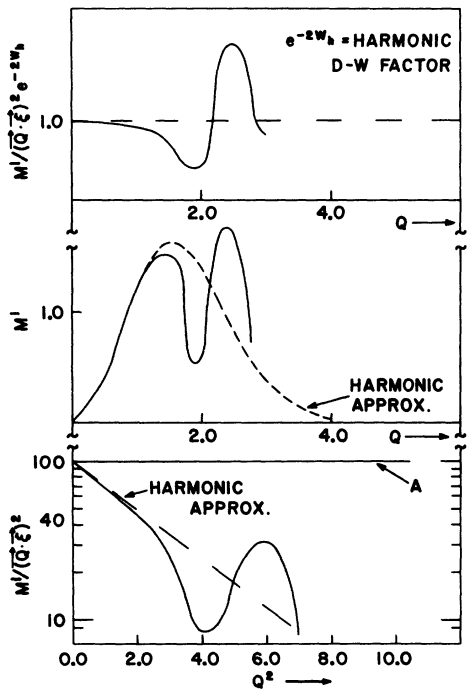

FIG. 4. Three equivalent ways in which the data for single-phonon scattering can be presented. The data are integrated by computer via the ACB sum rule. Line A in the bottom figure represents Placzek's sum rule.

at relatively larger wave vectors with poorer resolution, and were not included in the fit. A statistical weighting was used in the transverse branches to account for the difference in crystal mosaic. We note that the residuals given in Table I can be explained in terms of the observed non-Gaussian mosaic of the crystals. The results for the elastic constants are consistent with the data from our previous measurements and with Wanner's estimate from thermodynamic data.[13] The results given here are significantly more accurate than those in previous work.

The value for the initial slope of the $T_1[011]$ mode derived from these elastic constants is 163 ±30 m/sec. The results of a number of theoretical calculations for this branch suggest that the dispersion of this mode might be anomalous.[14] These calculations suggest that there could be a region at small wave vector for which the dispersion curve would have upward curvature. The derived value for the initial slope of this branch from the elastic constants strongly suggests that its dispersion is normal in that the slope is large enough to reach the zone boundary at 0.58 meV without upward curvature in the dispersion relation. One can speculate that, in view of the simple interatomic interaction between the helium atoms, the cubic phase of solid helium would satisfy the Cauchy relations for elastic isotropy in a cubic system, i.e., that $C_{12}=C_{44}$. The elastic constants determined from the results of this experiment clearly violate this relation. Assuming only a pair interaction, these results could suggest that the phonon spectrum is derived from an effective potential that is noncentral in character.

The results for the dispersion relation for bcc helium for a wider range of energy and propagation vector are given in Fig. 7. One of the important features of the data in the figure is that they do not cover the entire zone. The results for the higher-energy transfers, in contrast to those illustrated in Fig. 5, which are essentially similar to the groups observed from most crystals, were (a) generally broad, and (b) had profiles that were different at equivalent positions in reciprocal space. In the second zone, the groups were often severely distorted from the normal Gaussian-like spectral response. Unfortunately, the measurements for scattering vectors in the second Brillouin zone were usually in the transition region. Strictly speaking, therefore, the results for these higher-energy transfers can only be interpreted by convoluting a theoretical expression for the total scattering function. The shaded areas in the figure and the incomplete branches in the spectrum reflect our uncertainty both in being able to define a peak in these profiles and in deciding whether a given group was in fact scattering from a single excitation. The data in Fig. 7 are, we believe, the type that can be compared with theoretical results for the dispersion curves. The numerical results used to construct Fig. 7 are given in Tables II and III of the Appendix.

The solid lines in Fig. 7 represent a theoretical calculation for the spectrum by Glyde[15]; the lowest-

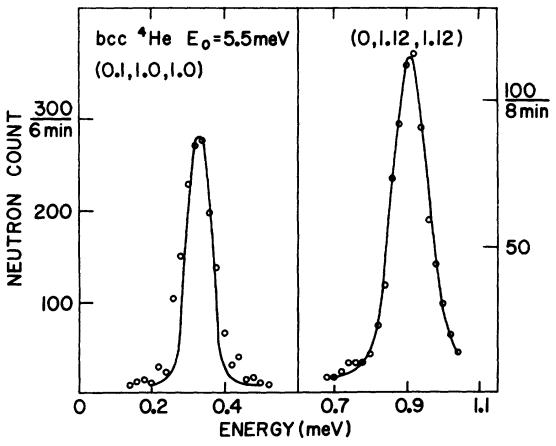

FIG. 5. Representative examples of two high-quality scans taken with high resolution. Data of the type shown in the figure were used to deduce the elastic constants and to quantitatively describe the effective Debye-Waller factor. The solid lines are a reproduction of a computer calculation of the convolution of the resolution function with an infinitely long-lived excitation.

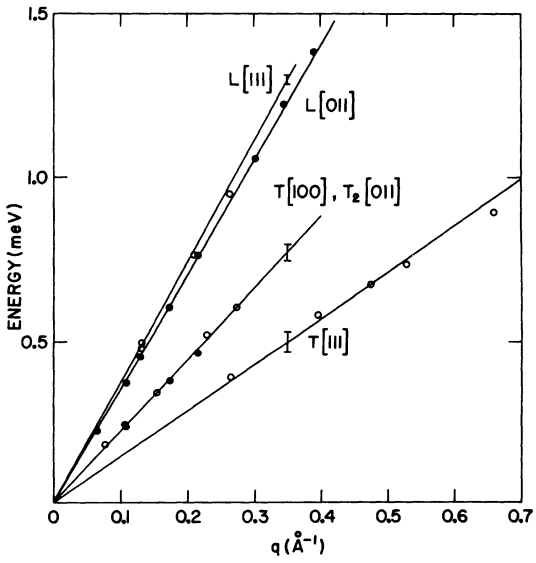

FIG. 6. Small-wave-vector portion of the dispersion relation of those branches that were used to obtain the elastic constants.

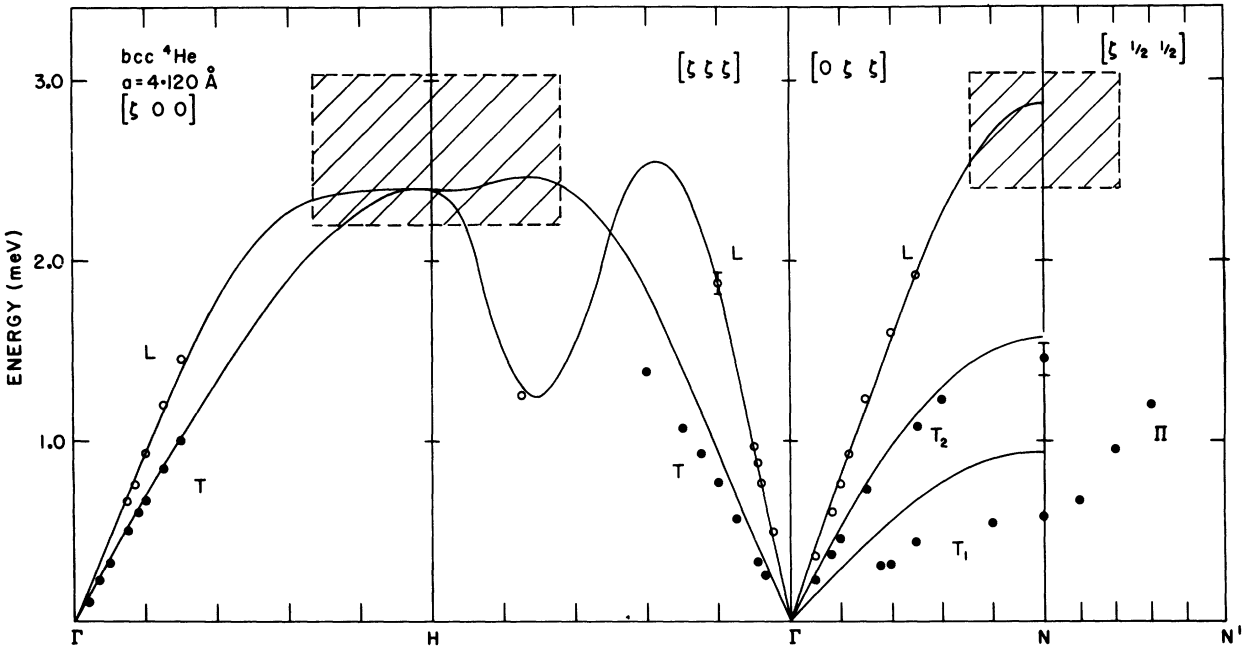

FIG. 7. Data for the dispersion curves of bcc helium. The cross-hatched regions illustrate those parts of the dispersion curves where there was an uncertainty in defining either a peak position in the group or an ambiguity in identifying the group as scattering from a single excitation.

order self-consistent phonon approximation was used in the calculation.

B. hcp Phase

Measurements were done in this phase to study the behavior of the cross section of those branches of the spectrum that were not observed in our earlier measurements, and to firmly establish whether the anomalous behavior of the cross section in this phase was similar to the one previously observed[4] for the bcc.

The results for the LO branch along the [001] direction are given in Fig. 8. The contours for the phonon profiles for this branch are reminiscent of those found in the bcc phase at the higher-energy transfers. An illustration of a profile observed for this branch is given in the top part of Fig. 9. The phonon group is very broad and is distorted from the Gaussian-like shape commonly observed for normal groups. As is expected, the data at this density for this branch show that the interference terms in the cross section for the hcp phase are as important as for the bcc. The shaded areas in Fig. 8 reflect the uncertainty in determining a "peak position" in the type of profile shown in Fig. 9.

The groups illustrated in the lower half of Fig. 9 are representative of the data that were taken for the modes with the normal profile. The TO mode is in good agreement with the original neutron-scattering experiments in this phase,[2] and with very recent results of light-scattering measurements.[16] The TO mode at the zone center was found to have an energy of 0.90 ±0.01 meV. The profiles on the lower left are examples of scans for the LA branch, and the solid lines are com-

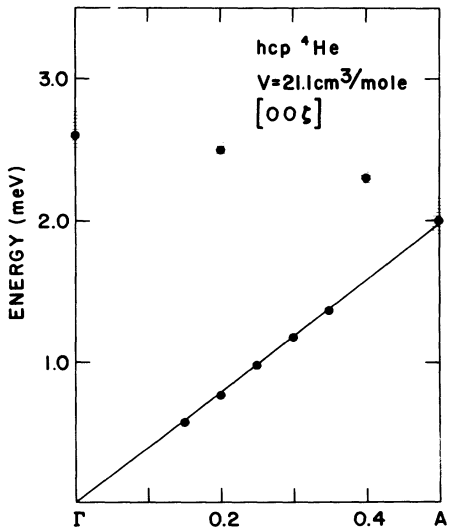

FIG. 8. Dispersion data for the LA and LO branches along the [00ζ] direction in the hcp phase. The cross-hatched areas illustrate the uncertainty in defining a peak position in the profile.

puter calculations for the line shape. The results show that the observed linewidth is caused primarily by the resolution of the instrument.

The data shown in Fig. 10 are the result of precise measurements along the [100] direction. The data that were used to construct the figure were taken primarily for the purpose of determining the cross section. Here we present only the results for the dispersion of these modes. The numerical data for these branches are given in Table IV of the Appendix.

IV. CROSS SECTION

We now discuss the scattering cross section in both phases of the solid. The experimental data presented in I showed that the scattering function in the bcc phase had an unexpected dependence on the magnitude of the scattering vector. The main effort of this experiment was to study the behavior of this unusual result in more detail.

At the outset, we note that the situation is more complex and more interesting than had been expected. To facilitate presenting the conclusions drawn from the data, we simplify the results and presume that the cross section can be easily divided into the scattering from single and multiple excitations. The latter is that part which merges with and becomes the single-particle excitations at large energy and momentum transfer. As was pointed out earlier, this assumption is not generally true, because in most cases the observations could not readily be identified as originating from either one source or the other. Nonetheless, the model is useful in describing the experimental results.

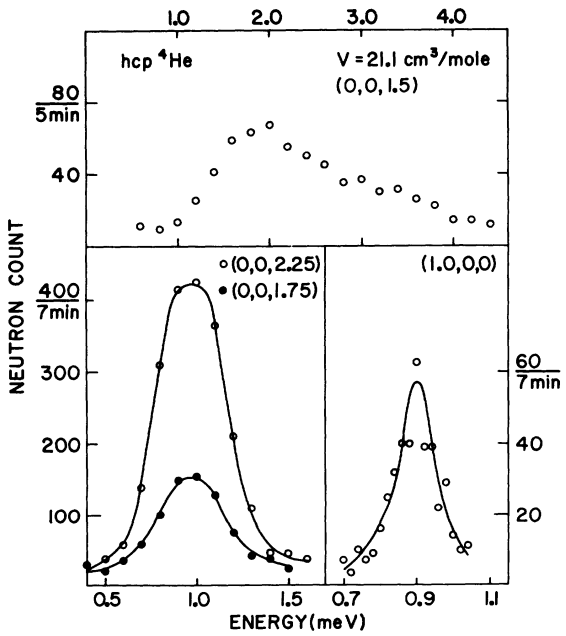

FIG. 9. Profiles of four groups for the hcp phase. The figure at the top illustrates the distorted profiles usually observed at higher-energy transfers. The bottom right is the scan for the TO branch at the zone center. The two groups at the lower left are scans at equivalent positions in reciprocal space and illustrate the unexpected intensity anomaly.

A. bcc Phase

We first present results for the cross section for those data which can be unambiguously identified as scattering from a single elementary excitation.

The essential feature of the dependence of this cross section on $|Q|$ is that it shows variations that are not expected from the classical form of the Debye-Waller factor. The data shown in Fig. 11 illustrate what is actually observed. The profiles on the bottom half are results taken at symmetry-related positions. The two groups are profiles of a LA [011] mode taken close to and on opposite sides of the (011) Bragg position. The top half illustrates what is expected from conventional theory at both positions. The cross section at the position *A should be* roughly 20% *smaller* than at *B*. However, in fact, one observes that the cross section at *A* is larger than at *B* by approximately a factor of 200%. The profiles of these groups, apart from their intensity, are identical to that usually observed in most solids. The profiles

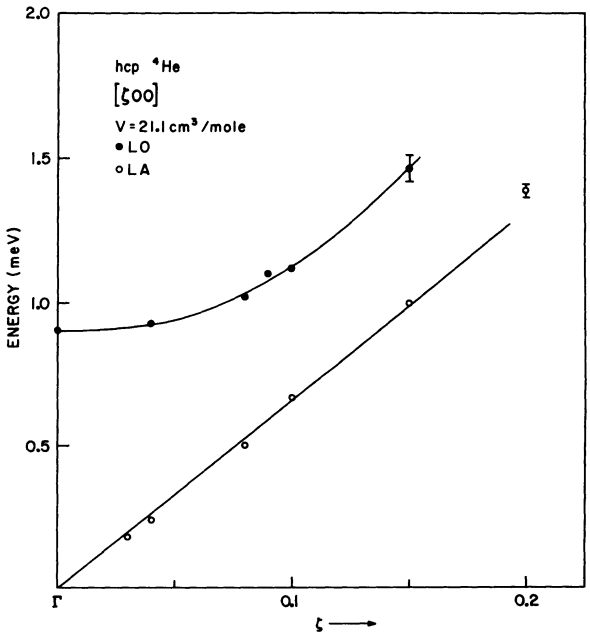

FIG. 10. Dispersion data for the LO and LA branches in the [ζ00] direction for the hcp phase.

are sharp and Gaussian-like. The solid lines in the figure are computer calculations for their line shape and show that their linewidths are primarily caused by instrumental resolution.

One of the conclusions given in I was that the anomalous behavior of the intensity was in some sense associated with the "appearance" of an additional cross section at an energy transfer ~1.4 meV (see, for example, the profiles given in Fig. 5 of I). The data in Fig. 11, and a great many other similar scans, show that this conclusion must be changed. It is now clear that the anomalous behavior of the cross section for single-excitation scattering has *no apparent connection with the energy transfer*. In effect, it can be divorced from the energy transfer, and appears to depend solely on the scattering vector.

The data illustrated in Fig. 11 were collected under conditions in which the instrument was operated with high resolution; i.e., the incident neutron energy was 5.5 meV. There is absolutely no ambiguity in the background scattering, and we can justifiably interpret the data as originating from a single elementary excitation in the usual sense. The behavior of this cross section as a function of the scattering vector cannot be studied with this incident energy for large scattering vectors, because of the restriction imposed by crystal momentum conservation. To have access to larger scattering vectors the incident energy was increased to 13.7 meV. The resolution of the instrument was increased by approximately a factor of 5 to maintain a reasonable signal-to-noise ratio. Unfortunately, with this poorer resolution one can no longer assume that the data are completely free from scattering due to multiple excitations. In fact, as is seen in the right-hand side of Fig. 3, the multiple-excitation and single-excitation scattering are of approximately equal magnitude for the energy and momentum transfer range covered with this incident energy.

In the present experiment we have identified those groups as scattering from an elementary excitation if (i) they were observed at energy transfers less than 1.1 meV, and (ii) they were taken under conditions in which the spectrometer was operated with high-energy resolution. After careful consideration, it was decided that selected

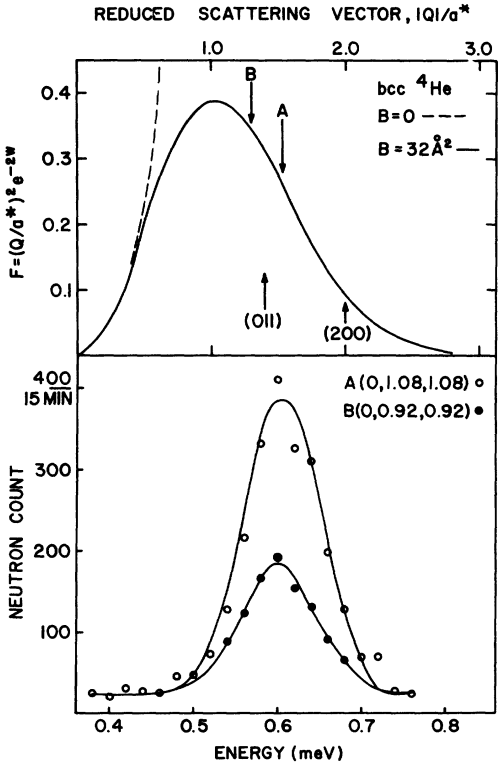

FIG. 11. Top part illustrates the normal Q dependence of the single-phonon cross section for solid helium from conventional theory. The bottom contains two groups taken at equivalent positions in reciprocal space in the bcc phase.

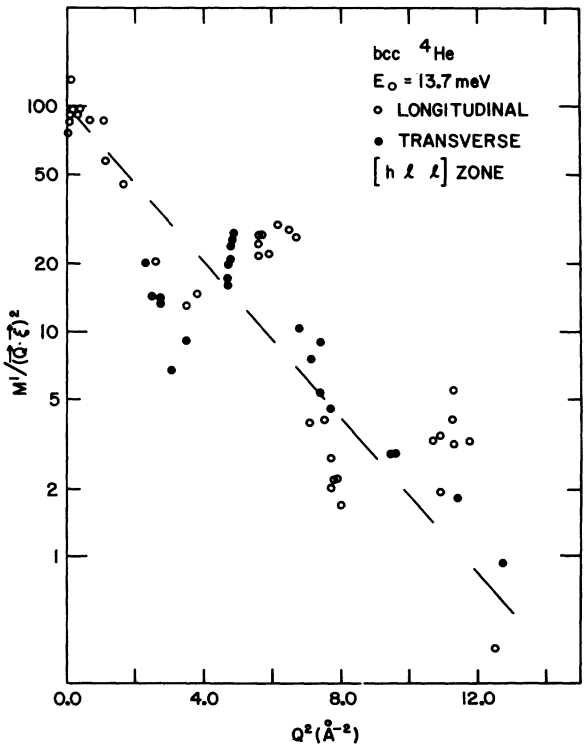

FIG. 12. Results of the effective Debye-Waller factor for bcc helium. The results are a qualitative description; a quantitative description is given in Fig. 14. Two oscillations are present in the data. The dashed line is the result expected from conventional theory.

scans at low resolution could *qualitatively* describe the single-excitation cross section. A *quantitive* description, on the other hand, can only be obtained with confidence with the high-resolution results. The data for the quantitive description of the cross section for single-excitation scattering used results essentially similar to those given in Fig. 5 and the profiles in Fig. 11.

The intensity data taken with the lower resolution are illustrated in Fig. 12. The quantity $M^1/(\vec{Q}\cdot\vec{\xi})^2$ is plotted on a log scale versus Q^2. If the data were consistent with the ACB sum rule, which they should be for weakly anharmonic systems, the data would lie on a straight line, the slope of which would determine the quantity $B = 3\hbar^2/2Mk\Theta_D$, where Θ_D is the Debye temperature and B is defined by the Debye-Waller factor $|d(\vec{Q})|^2 = e^{-2B(Q/4\pi)^2}$. The dashed line in the figure is the calculated slope for bcc helium using $\Theta_D = 22.5°\text{K}$.[17] It is clear that the observed Debye-Waller factor, or structure factor, displays oscillations about the expected result. The errors in the measurement are illustrated by the scatter in the data. The data were collected for scattering vectors in the $[0\bar{1}1]$ zone and, in this zone to within experimental accuracy, they lie on a universal curve that depends only on $|Q|$. The figure contains representative results from all branches in the phonon spectrum along the principal symmetry directions that can be observed in this zone. We choose not to distinguish between branches, and refer only to the polarization vector of the mode. We also point out that the data in the figure are a composite of results taken on five different crystals. The data were consistent from one crystal to the next.

The lowest transverse mode T_1 along the [011] direction can be observed only at the N point in the $[0\bar{1}1]$ zone. The results of experiments on this mode for a crystal oriented in a [100] zone are shown in Fig. 13. The dashed line is again the expected slope with $\Theta_D = 22.5°\text{K}$. The two data points with $Q^2 > 12.0$ Å^{-2} were taken on crystals in the $[0\bar{1}1]$ zone, and were included in this figure to compare theory and experiment over a wider range in Q. The important feature of these data is that, surprisingly, the data in this zone do not show the oscillatory behavior observed in the other. They behave normally, and we conclude that the effective Debye-Waller factor for bcc helium depends not only on the magnitude of the scattering vector but also on its direction.

The data which quantitatively reflect the effective Debye-Waller factor for bcc helium are given in Fig. 14. The quantity $M_i^1(\vec{Q})/(\vec{Q}\cdot\vec{\xi}^i)^2 e^{-2W_h}$ is plotted versus Q. If the data were consistent with

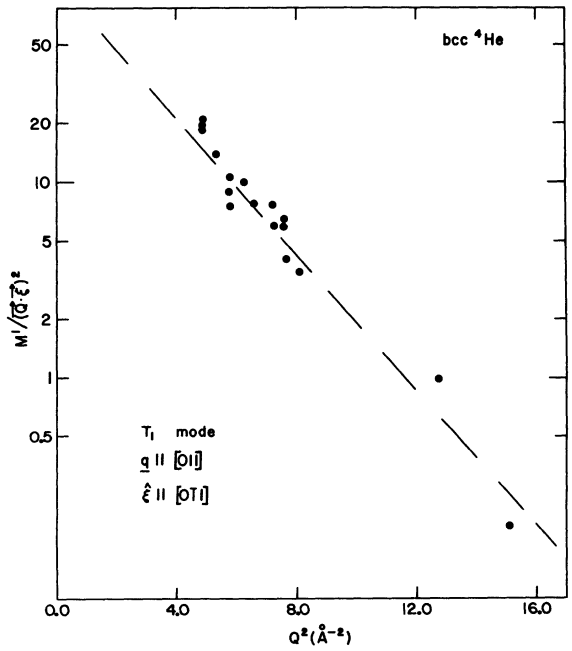

FIG. 13. Results for the T_1 mode. As is obvious, the data taken for this mode behave in the normal manner. The data were collected in the [100] zone.

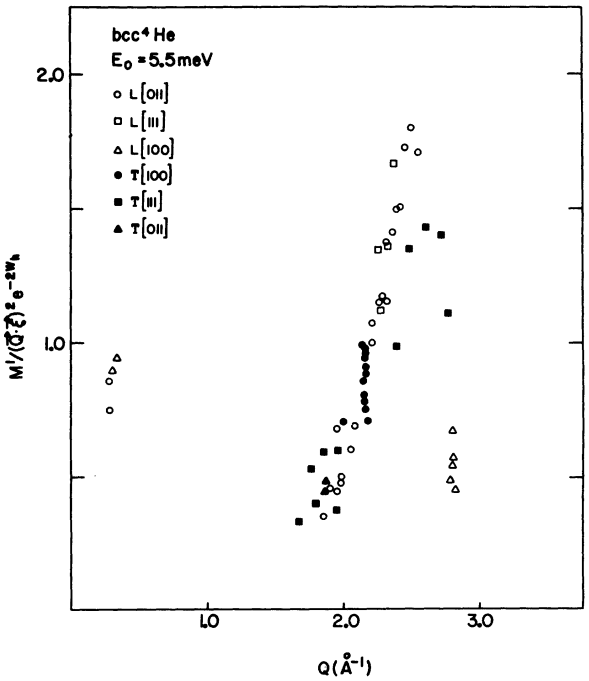

FIG. 14. Quantitative description of the first oscillation in the effective Debye-Waller factor for bcc helium. High-resolution data collected with an incident energy of 5.5 meV were primarily used to construct the figure. We believed that these data are esentially free of multi-excitation contamination.

the ACB sum rule, i.e., if the Gaussian approximation were correct, the data would be independent of Q, and lie on the straight line $M_1^1(\vec{Q})/(\vec{Q}\cdot\vec{\xi}^i)^2 e^{-2W_h} = 1.0$. The first oscillation shown in Fig. 12 is clearly visible. The second oscillation in Fig. 12, on the other hand, could not be studied with the high resolution for reasons given earlier. The four points for $Q \sim 0.2$ Å^{-1} are carefully selected data taken in forward scattering with the incident energy of 13.7 meV. They were taken in the first Brillouin zone at scattering vectors for which the single-phonon cross section continues to dominate Placzek's[12] sum rule. The purpose for including these data is a very important one: They serve to establish the $Q=0$ limit for the abscissa.

B. hcp Phase

Preliminary measurement in the hcp phase by Osgood *et al.*[4] showed that the scattering cross section was anomalous. Experiments were therefore done in this phase in order to compare more precise results with those previously obtained for the bcc phase. The experiments were done on crystals with a molar volume of 21.1 cm^3/mole, which is the same as in our previous measurements. The results show that the behavior of the cross section for single-excitation scattering is very much the same in both phases. The results for the hcp phase are given in Fig. 15. The data in the figure should be compared with those for the bcc crystals given in Fig. 12.

The bottom-left profiles in Fig. 9 are representative examples of data taken at equivalent positions on either side of the (002) Bragg position. In other words, the data were taken on the same mode; the only difference is that the scattering vectors are different. The same kinds of arguments that were used for the profiles in Fig. 11 for the bcc phase are applicable to these profiles. Conventional theory would dictate that the cross section at the (0, 0, 2.25) position be smaller than at the (0, 0, 1.75). In fact, the observations show that the opposite is true. The cross section at the larger scattering vector is approximately a factor of 3 too large.

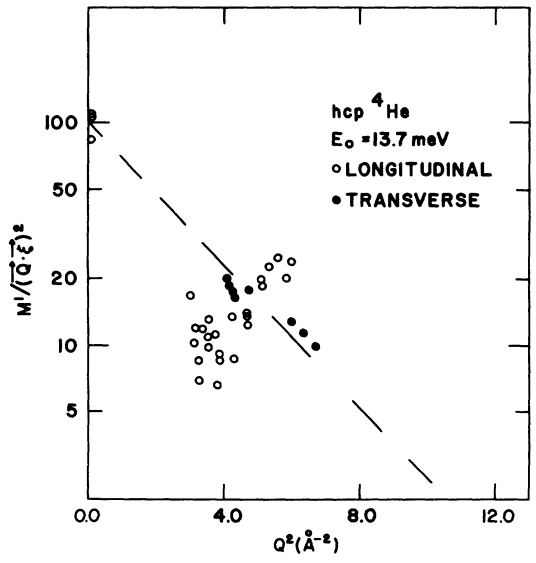

FIG. 15. Results for the effective Debye-Waller factor for the hcp phase. The data should be compared with those given in Fig. 12.

There are two atoms in the primitive unit cell in the hcp phase, and it might be argued that this reversal in the intensity reflects the dependence of the inelastic structure factor on the scattering vector. For the c^* direction, however, the inelastic structure factor for the phonon modes is independent of the scattering vector, and is fixed by symmetry to be 2.0. For directions in the hcp phase other than c^*, the inelastic structure factor for each mode is $\vec{Q}$ dependent. To utilize the intensity data for these directions, in our case the [100], one can use a sum rule on the structure factors which states that $\sum_j F_j^2(Q) = \text{const}$, where $F_j(\vec{Q})$ are the inelastic structure factors for the j branches that can be observed in a given scan. Stated differently, in a given scan for either the transverse or longitudinal branches, the sum of the intensities over all the phonon branches that can be observed in the scan is independent of the individual inelastic structure factors and therefore of the Q dependence contained therein. This procedure was followed for the data along the [100] direction.

V. SINGLE-PARTICLE SCATTERING

Measurements were done for large scattering vector and high-energy transfers to study the structure of the scattering function for a quantum crystal at energy transfers well above the top of the phonon spectrum.[11] The experiments were performed on a multicrystal in the hcp phase and along the [111] and [100] directions in the bcc phase. Figure 16 contains some representative results collected in this scattering regime. The results show that there exist well-defined groups for very-high-energy transfers. Their dispersion relation is isotropic and apparently independent of the crystallographic phase. More important, the scattering from the solid in this regime is practically identical to the results obtained for the superfluid phase by Cowley and Woods.[18] The profiles labeled (b) in Fig. 16 are data taken from Cowley and Woods,[18] and should be compared with

the other profiles in the figures taken for the solid. Cowley and Woods[18] argue that, for the liquid, for scattering vectors $\vec{Q} > 3.0$ Å^{-1} the groups represent essentially scattering from single-particle excitations. Our new data suggest that very similar single-particle states exist in the solid. The intrinsic linewidths of these groups are not inconsistent with a lifetime limited by a collision with nearest neighbors. These results show that the dynamics of the superfluid liquid and the solid on the scale of this time and distance are quite similar.

The results for the dispersion relation for these states are given in Fig. 17. The free-particle dispersion relation for a ^{4}He atom is given by the solid line in the figure. The experimental results show that the helium atom in the solid can be considered "dressed," the observed effective mass being $M^* = 1.27M_4$, where M_4 is the mass of the free atom. The dashed lines in the figure show the positions of the half-width at half-maximum (HWHM) of the observed neutron groups.

VI. COMMENTS

A. Elementary Excitations

The data that were used to construct the dispersion curves for solid helium in this paper were limited to the lowest-lying sharp resonant structure in the scattering function. Throughout the discussion, these data were referred to as scattering from the "elementary excitations," rather than the more commonly used phrase "single-phonon scattering." The reason for using the more general term was motivated by Horner's[19] recent theoretical work. Horner[19] has shown that the contribution made by the interference terms is extremely important for the quantum solids of

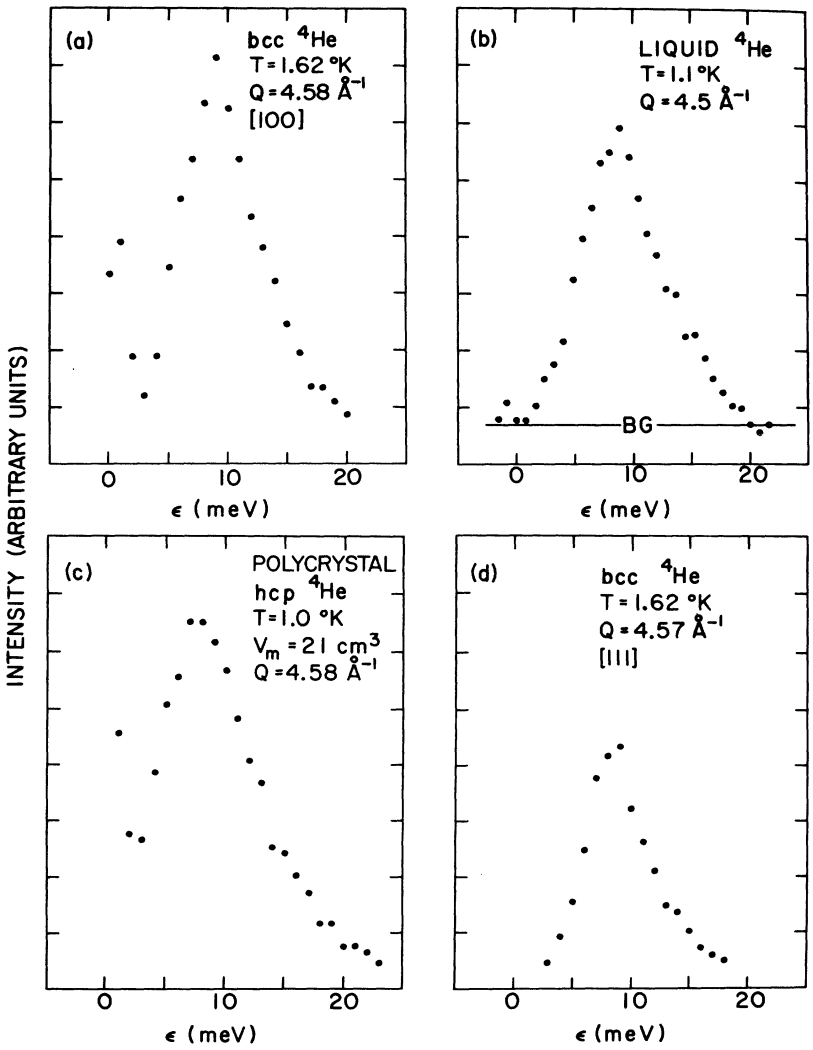

FIG. 16. Representative group of high-energy single-particle scattering. The essential feature of this cross section is that it is identical to that observed in the superfluid phase.

helium—so much so that the character of the excitation is severly altered. In contrast to the model of the elementary excitation in a harmonic or weakly anharmonic crystal, in which the atom, (more precisely the distribution of the atom about its equilibrium position) oscillates rigidly, the density distribution itself distorts during the motion. The elementary excitation in effect becomes a coupled mode. It is an admixture of a purely displaced mode and another that distorts the width of the distribution to accommodate the displacement. This distortion is associated with two phonon processes. In other words, the excitation is not solely a "phonon," that is, a resonance in the displacement-displacement correlation function. The theoretical results[19] show that the spectral response of this elementary excitation or "physical phonon"[19] is similar to the response observed in normal systems in that it can be characterized by a well-defined peak and is generally the lowest-lying excitation in the system. As was mentioned previously, the data given for the phonon dispersion in this paper are associated with the lowest-lying peak observed in the scattering function at small-energy transfer. For convenience, we shall now refer to this structure as phonon scattering, keeping in mind that the phrase is used in a more general sense than is normally done.[19]

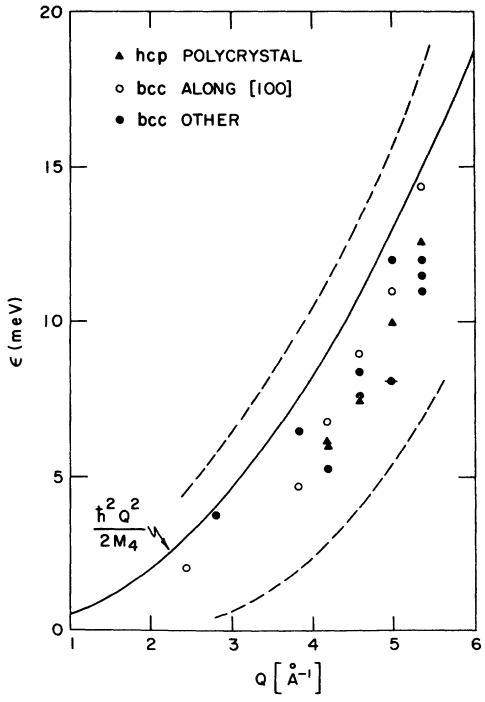

FIG. 17. Results for high-energy scattering. The free-particle dispersion curve for the ^{4}He atom is given by the solid curve.

The most striking feature of the data collected for these excitations is that their scattering function is not consistent with the ACB sum rule. An effective Debye-Waller or structure factor was constructed from the data. This structure factor is decidedly non-Gaussian, and displays oscillations as a function of $|Q|$. The branches in the three principal symmetry directions were studied. The scattering functions for all of the branches, except the lowest transverse mode T_1 along the [011], were found to have this unusual dependence on the scattering vector.

We emphasize that, apart from its dependence on $|Q|$, the structure of the scattering function for these excitations is similar to those observed in ordinary materials. A theory that purports to explain the anomalous behavior of the first moment of these groups must specifically reproduce data of the type given in Fig. 11. However, we note that the data are not inconsistent with the results of Refs. 7–9, 19, and the early work by Gillessen and Biem,[20] because these calculations are based on an unmeasurable quantity for arbitrary $\vec{Q}$, namely, that part of the scattering function due to displacive motions only.

There is one possible source of confusion with regard to the interpretation of these experimental results. The first conclusion that one can draw from the data is that the probability distribution of a given atom about its equilibrium position is anisotropic and non-Gaussian. One is immediately tempted to Fourier invert the data to obtain this distribution function. This inversion can be misleading. A Fourier inversion of the data given in I was recently attempted by McMahan and Guyer.[8] They concluded that the data implied a nonphysical negative distribution for $R \sim 2.0$ Å. This nonphysical behavior is an artifact of the Fourier inversion itself. Our own early efforts to invert the data at first yielded similar results. It soon became clear, however, that equally reasonable, and perhaps better, fits to the data eliminated the region of negative density. The details of these calculations are presented in a separate publication.[21] The proper way to compare theory and experiment is not by comparing the Fourier-inverted density distribution obtained from the data, but rather by calculating the Debye-Waller factor from the theoretical models and then comparing the results directly with experiment.

There have been recent theoretical attempts to reproduce the observed effective Debye-Waller factor for solid helium using different approximations. Sears and Khanna[7] used the Jastrow-Hartree approximation. Their calculation failed to agree with the experimental results given in I. They therefore concluded that the manner in which the data were analyzed

was in error. In particular, they asserted that the high-energy wings of certain phonon groups were handled improperly. The data given in Figs. 9 and 11 are conclusive, and show that the unusual behavior of this cross section is characteristic of the solid. Horner[9] has improved the SCH calculation. His results are also not in agreement with experiment.

B. Transition Region

The results in this region are at the moment difficult to interpret. The proper way to analyze the results is by convoluting the spectrometer resolution function with a theoretical expression for the *total* scattering function. It appears[19] that calculations of this type will be available in the near future. The detailed comparison between theory and experiment in this region will be especially interesting.

There is one feature of experiments done in this region that must be understood. The identification of the single-phonon component of the scattering function in this region can then be easily masked and dominated by the multiphonon contribution. We emphasize that one must exercise extreme care in identifying those neutron groups from solid helium that are collected in the higher-energy region of the phonon spectrum. There have been experiments performed in the hcp phase of helium on crystals with a molar volume of 16.0 cm^3/mole by Reese *et al.*[3] Their measurements contain evidence for the existence of "anomalous neutron groups" at this molar volume. These anomalous groups are probably the counterpart of the multiphonon scattering observed at that density. Reese *et al.*[3] pointed out that, when one compares the phonon spectrum of the earlier work in the hcp phase at 21.1 cm/mole and their own results, the phonon energies scale rather well by a factor of 1.9. The new results given in Fig. 8 indicate that this scaling may break down for the LO branch, which scales by 2.6. However, it is possible that the groups that they indicate at the higher energies for the LO branch along c^* have been incorrectly identified, and are in fact not single-phonon scattering but multiple-phonon peaks (see, for example, Fig. 3 of Reese *et al.*). We suggest that further work is necessary to establish whether this scaling in fact exists.

C. Single-Particle Scattering

The experiments that were done for energy transfers above the top of the phonon spectrum reveal that the dynamics of these solids at these energies are essentially similar to a free particle contained within a Wigner-Seitz cell. We have directly observed for the first time single-particle excitations in a solid. The dispersion relation for these excitations is independent of the crystallographic phase, and is consistent with an effective mass $M^* = 1.27 M_4$. The lifetime for these excitations is consistent with nearest-neighbor collisions. The data for these excitations are practically identical to the results obtained by Cowley and Woods[18] for the superfluid. These measurements suggest that the dynamics of solid and superfluid helium for energies above the phonon spectrum are very similar.

D. Concluding Remarks

Over-all, the main result of these experiments is that they have established the general features of the scattering function of a quantum solid over a wide range of energy and momentum transfer. The transition from the region wherein the single-phonon excitations dominate the scattering function to the single-particle regime at high-energy transfers has been documented in some detail. There remains a great deal more work to be done in the quantum region of the phase diagram of solid helium. It would appear that a more thorough and extensive study of the single-particle scattering will prove rewarding. The solids in this region are unique; they will continue to yield new, exciting results that may greatly modify our current concepts of the lattice excitations of a quantum solid.

ACKNOWLEDGMENTS

We would like to express our thanks to T. Oversluizen and M. Rosso for their expert technical assistance. The many conversations with our colleagues N. R. Werthamer, T. Koehler, H. R. Glyde, H. Horner, M. Blume, P. P. Craig, V. J. Emery, F. P. Lipschultz, L. Passell, V. Korenman, and R. Prange are greatly appreciated.

APPENDIX

TABLE I. Elastic constants for bcc ^{4}He in units of 10^4 m^2/sec^2 for $T = 1.620 \pm 0.005$°K and lattice constant $a = 4.120$ Å.

	C_{11}/ρ	C_{12}/ρ	C_{44}/ρ
This expt.	18.3 ± 0.8	15.6 ± 0.5	11.3 ± 0.4
Osgood *et al.* (Ref. 4)	17.7 ± 3.2	15.8 ± 3.5	10.7 ± 1.0
Wanner (Ref. 13)	17.3 ± 2.6	15.2 ± 2.6	12.3 ± 0.5

TABLE II. Experimental values for the phonon energy for the $(\zeta, 0, 0)$ and (ζ, ζ, ζ) directions for bcc He with $a = 4.120$ Å at $T = 1.620 \pm 0.005$°K.

$L(\zeta,0,0)$		$T(\zeta,0,0)$	
ζ	E(meV)	ζ	E(meV)
0.15	0.67 ± 0.04	0.05	0.173 ± 0.007
0.16	0.67 ± 0.04	0.07	0.241 ± 0.007
0.17	0.76 ± 0.04	0.10	0.341 ± 0.007
0.18	0.79 ± 0.03	0.15	0.521 ± 0.007
0.20	0.94 ± 0.04	0.18	0.604 ± 0.006
0.22	1.04 ± 0.04	0.20	0.681 ± 0.012
0.25	1.20 ± 0.03	0.25	0.85 ± 0.05
0.3	1.45 ± 0.14	0.3	1.00 ± 0.05
$L(\zeta,\zeta,\zeta)$		$T(\zeta,\zeta,\zeta)$	
0.05	0.49 ± 0.006	0.07	0.255 ± 0.012
0.08	0.773 ± 0.007	0.09	0.336 ± 0.019
0.09	0.874 ± 0.008	0.10	0.386 ± 0.012
0.10	0.950 ± 0.008	0.15	0.578 ± 0.012
0.20	1.87 ± 0.05	0.20	0.775 ± 0.016
		0.25	0.925 ± 0.016
		0.30	1.082 ± 0.018
		0.40	1.38 ± 0.04

TABLE III. Experimental values for the phonon energy for the $(0, \zeta, \zeta)$ and $(\zeta, \frac{1}{2}, \frac{1}{2})$ directions for bcc ^{4}He with $a = 4.120$ Å at $T = 1.630 \pm 0.005$°K.

$L(0,\zeta,\zeta)$		$T_1(0,\zeta,\zeta)$	
ζ	E(meV)	ζ	E(meV)
0.03	0.212 ± 0.006	0.18	0.31 ± 0.03
0.05	0.368 ± 0.006	0.20	0.32 ± 0.05
0.08	0.605 ± 0.006	0.25	0.44 ± 0.03
0.10	0.769 ± 0.008	0.4	0.55 ± 0.04
0.12	0.909 ± 0.006	0.5	0.58 ± 0.03
0.13	1.00 ± 0.03		
0.14	1.06 ± 0.03		
0.15	1.22 ± 0.05		
0.16	1.22 ± 0.03		
0.18	1.38 ± 0.03		
0.2	1.60 ± 0.03		
0.25	1.92 ± 0.04		
$\Pi(\zeta,\frac{1}{2},\frac{1}{2})$		$T_2(0,\zeta,\zeta)$	
0.7	1.2	0.05	0.235 ± 0.007
0.8	0.927	0.08	0.38 ± 0.01
0.9	0.659	0.10	0.46 ± 0.01
		0.15	0.73 ± 0.04
		0.25	1.09 ± 0.04

TABLE IV. Experimental values for the phonon energy for the LO and LA branches for hcp ^{4}He near the zone center with lattice constants $a = 3.671$ Å and $c = 6.013$ Å for $T = 1.4$°K.

ζ	LA	LO
0.0		0.90 ± 0.01
0.03	0.177 ± 0.006	
0.04	0.240 ± 0.004	0.93 ± 0.01
0.08	0.50 ± 0.01	1.02 ± 0.02
0.9		1.11 ± 0.02
0.10	0.67 ± 0.02	1.12 ± 0.02
0.15	0.99 ± 0.02	1.47 ± 0.09
0.20	1.39 ± 0.03	2.06 ± 0.18

*Work supported by the U. S. Atomic Energy Commission.

†Partially supported by the Advanced Research Projects Agency and National Science Foundation.

[1]N. R. Werthamer, Am. J. Phys. 37, 736 (1969), and references contained therein.

[2]V. J. Minkiewicz, T. A. Kitchens, F. P. Lipschultz, and G. Shirane, Phys. Rev. 174, 267 (1968). Also, F. P. Lipschultz, V. J. Minkiewicz, T. A. Kitchens, G. Shirane, and R. Nathans, Phys. Rev. Lett. 19, 1307 (1967).

[3]R. A. Reese, S. K. Sinha, T. O. Brun, S. K. Sinha, and C. R. Telford, Phys. Rev. A 3, 1688 (1971); T. O. Brun, S. K. Sinha, C. A. Swenson, and C. R. Tilford, in *Neutron and Inelastic Scattering VI* (International Atomic Energy Agency, Vienna, 1968).

[4]E. B. Osgood, V. J. Minkiewicz, T. A. Kitchens, and G. Shirane, Phys. Rev. A 5, 1537 (1972).

[5]V. Ambegaokar, J. M. Conway, and G. Baym, J. Phys. Chem. Solids Suppl. 1, 261 (1965); in *Proceedings of*

the International Conference on Lattice Dynamics (Pergamon, New York, 1965).
[6]N. R. Werthamer, Phys. Rev. Lett. 28, 1102 (1972).
[7]V. F. Sears and F. C. Khanna, Phys. Rev. Lett. 29, 549 (1972).
[8]E. McMahan and R. Guyer, in Proceedings of the Thirteenth International Low-Temperature Physics Conference, Boulder, 1972 (unpublished).
[9]H. Horner, J. Low Temp. Phys. 8, 511 (1972).
[10]T. A. Kitchens, G. Shirane, V. J. Minkiewicz, and E. B. Osgood, Phys. Rev. Lett. 29, 552 (1972).
[11]M. Rosso and T. Oversluizen (unpublished).
[12]G. Placzek, Phys. Rev. 86, 377 (1952).
[13]R. Wanner, Phys. Rev. A 3, 448 (1971).
[14]H. Horner, Phys. Rev. Lett. 25, 147 (1970).
[15]H. R. Glyde, J. Low Temp. Phys. 3, 559 (1970), and private communication based on H. R. Glyde, Can. J. Phys. 49, 761 (1971).
[16]R. E. Slusher and C. M. Surko, Phys. Rev. Lett. 27, 699 (1971).
[17]B. J. Alder, W. R. Gardner, J. K. Hoffer, N. E. Phillips, and D. A. Young, Phys. Rev. Lett. 21, 732 (1966); J. K. Hoffer, Ph.D. thesis (University of California, Berkeley, 1968) (unpublished).
[18]R. Cowley and A. D. B. Woods, Can. J. Phys. 49, 177 (1971).
[19]H. Horner, Phys. Rev. Lett. 29, 556 (1972).
[20]P. Gillessen and W. Biem, Z. Phys. 216, 499 (1968).
[21]T. A. Kitchens, in Ref. 8.